Sensors and Materials, Vol. 12, No. 7 (2000) 421--434
MYU Tokyo

S & M 0419

Research Trends in Infrared Detection in BAE SYSTEMS: Cadmium Mercury Telluride, InSb and Pyroelectric Arrays

P. Capper, L. G. Hipwood, P. Knowles, C. D. Maxey and A. D. Parsons

BAE SYSTEMS Infra-Red Limited, P. O. Box 217, Millbrook, Southampton, SO15 0EG, UK

(Received July 18, 2000; accepted November 4, 2000)

Key words: CMT, InSb, pyroelectric, LPE, MOVPE, long linear arrays, 2D arrays, heterostructures

Progress in the development of detectors for infrared imaging has been very rapid in recent years. In the year 2000, the range of detectors in service spans three 'generations,' from the older photoconductive cadmium mercury telluride (CMT) detectors in two-dimensionally scanned imagers, through one-dimensionally scanned long linear CMT detectors, to two-dimensional staring arrays with full TV resolution. In addition, uncooled detector technology has matured and opened up a host of new applications for low-cost staring arrays. This rapid progress has been achieved in cooled detectors through the introduction of improved epitaxial growth techniques for semiconductor crystals, diverse device structures and processes, and novel multiplexer designs. Uncooled detector technology has progressed in particular through the development of improved microbridge structures and thermally sensitive materials. This paper describes the major topics of materials research at BAE SYSTEMS Infra-Red Limited which are enabling the introduction of new detector products for the most advanced thermal imagers. The major topics covered are CMT growth by LPE and MOVPE, novel InSb devices grown by MBE, and pyroelectric arrays in lead zirconate titanate and lead scandium tantalate.

1. Introduction

The search for affordable detectors, combined with the highest quality and performance has generated some novel materials strategies at BAE SYSTEMS Infra-Red, which are outlined in this paper.

The present state of infrared imaging may be likened to having the entire evolutionary span of conventional television in production at the same time, employing everything from moving mirrors to large format solid-state arrays. The television analogy also applies to the infrared endpoint: large staring arrays and the possibility of uncooled operation in the thermal infrared wavebands.

At the level of the single detector element, cadmium mercury telluride (CMT) detectors, cooled to liquid air temperature, have demonstrated photon-noise-limited performance for at least 20 years. The achievement of higher sensitivity in the thermal image has become possible only by increasing the element count in detector arrays. While this development route has led to simpler optomechanical design in second-generation imagers, leading ultimately to the elimination of moving parts in the third-generation, the degree of difficulty in detector manufacturing has increased, through the introduction of multiplexers to constrain the number of wire connections, the replacement of photoconductors by photodiodes to suit the multiplexer interface and limit power dissipation, and through increased demands for affordable, large-area, uniform, low-defect, semiconductor crystal growth. This paper concentrates on the semiconductor materials technology for large but affordable detector arrays.

The possibility of very high performance combined with uncooled operation has arisen through use of microbridge bolometer arrays, which introduced new materials and engineering challenges. Among all the uncooled detector materials, the pyroelectric materials lead zirconate titanate and lead scandium tantalate offer potentially the highest performance.

2. Liquid Phase Epitaxy

In common with other suppliers, our approach to long linear detector arrays uses CMT grown by liquid-phase epitaxy (LPE), which produces high-quality long-wave diodes. LPE also provides high-quality medium-wave arrays, although with the limitation that the small dimensions and relatively high cost of the cadmium zinc telluride substrates have stimulated a search for alternative growth techniques and materials for larger scale epitaxy at lower cost.

Current requirements are typically for single pieces of device quality CMT up to 17.5×2 mm for long linear arrays and 6×8 mm for 2D. The LPE process is based on a tellurium-rich melt and the use of high-quality CdZnTe substrates, both 20×30 and 20×40 mm in size. Control over the impurity levels in the major constituent elements is a crucial part of the overall process. The growth solution and HgTe overpressure source are made from high-purity elements: the tellurium is zone-refined in hydrogen and the mercury is distilled immediately prior to use.

Growth takes place in a high-purity graphite boat in flowing Pd-diffused hydrogen (see Fig. 1). The long component is the moving section, or 'slider,' and it has a precisely machined well in which the prepared substrate is placed. Resting directly on this section is the melt holder which has two large through-wells for growth and annealing, and a third blind well between them. The latter holds the HgTe source which provides the necessary Hg overpressure control during growth. Growth occurs by ramp cooling from ~500°C (at

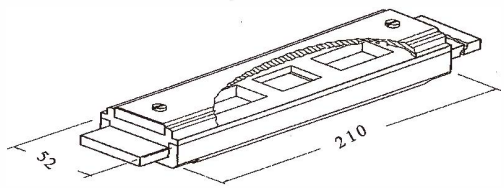

Fig. 1. LPE graphite boat design, dimensions in mm.

2 or 3°C h^{-1}) to produce layers with thicknesses between 25 and 35 μm. The temperature during growth must be controlled to within 0.2°C. Following wipe-off of the melt, an *in situ* anneal at ~300°C is used to set the acceptor concentration to the level required for photodiode fabrication (in the range of 1×10^{16} to 3×10^{17} cm^{-3}).

Assessment of the layers includes Fourier transform infrared (FTIR) spectrometry to map the lateral variations in wavelength and thickness (see Fig. 2). The cut-on wavelength of the material is controlled by its composition, expressed as x in $Cd_xHg_{1-x}Te$. The composition of the layer is, in turn, controlled by the composition of the melt close to the growth interface, and the segregation coefficients of the elements across the growth interface.[1] By adjusting the composition of the melt, the composition of the layer can be tuned to medium (3–5 μm) or long wavelength (8–12 μm). There is also a grade in x through the thickness of the layer and this must be determined and allowed for during device processing (see Fig. 3). This depth profile is measurable by Auger electron spectroscopy (AES) on a chemically bevelled sample.

A further measure of the quality of the LPE layers is the background donor level. Isothermal annealing of the CMT in a mercury atmosphere reduces mercury vacancies. The electrical properties are then controlled by the presence of residual impurities. This level is determined by Hall effect measurements. Levels of $< 1\times10^{15}$ cm^{-3} are normally required for photodiode arrays, while lower levels ($< 4\times10^{14}$ cm^{-3}) are necessary in order to fabricate the highest performance photoconductive devices, and both of these are routinely achieved.

Layer morphology is influenced by edge effects, substrate flatness prior to growth, and control of the growth rate. A 30-μm-thick layer usually has a 1-mm-wide edge zone of enhanced growth, all of which is removed during device processing. Flatness measurements reveal typical variations of ~ ±5 μm over a 2×4 cm LPE layer, with the majority of this confined to the corners.

To fabricate devices, the top 10 μm of a layer is removed to planarise the surface, then the substrate is removed by etching and the layer further polished to produce a 10-μm-thick 'monolith' which forms the detector array component. This is glued directly to the multiplexer chip to form a uniformly bonded 'membrane' that accommodates the thermal expansion of the silicon through elastic strain. This unique approach to array manufacturing combines the ability to fabricate very long or large arrays from a single array component (no butting) with a very stable and robust device structure, capable of withstanding thermal cycling without degradation.

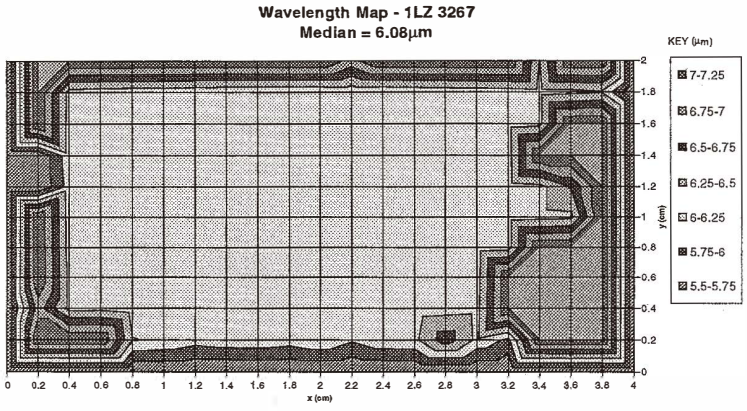

Fig. 2. Wavelength map of long wavelength 2×4 cm LPE layer.

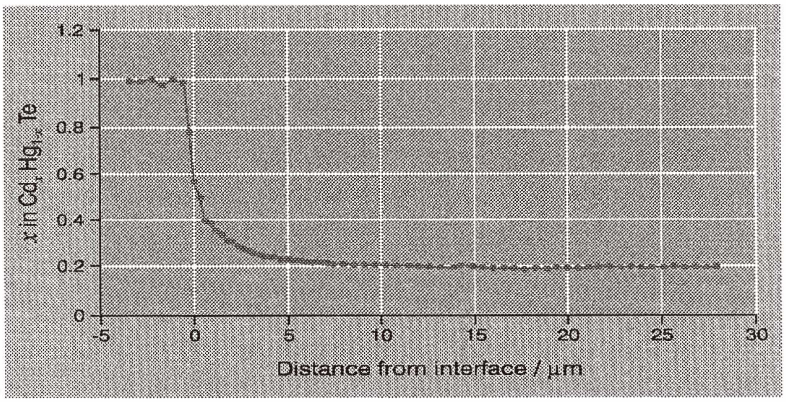

Fig. 3. Composition through the thickness of an LPE layer by AES.

3. CMT by Metalorganic Vapour Phase Epitaxy

Whereas LPE supplies second-generation detector arrays in the form of long linear arrays and small 2D arrays, the cost issues surrounding this growth technique have stimulated the search for some alternatives.

The metalorganic vapour phase epitaxy (MOVPE) growth technique involves the thermal pyrolysis of metal alkyl molecules, of the form $(R)_n$-M (where M is a metal atom, R represents organic bonded subgroups and n is the metal valency). Elimination of the organic side groups leaves metal atoms available on the substrate surface which, when growth conditions are ideal, will incorporate epitaxially into the crystalline lattice presented by the substrate.

The growth temperature is constrained by the thermal stability of the metal alkyls. Di-iso propyl tellurium (DiPTe) allows a growth temperature of ≈ 350°C. The cadmium

source, di-methyl cadmium (DMCd), readily decomposes at even lower temperatures (≥200°C). Sufficiently large Hg overpressures required for CMT growth cannot be provided by a mercury alkyl and so mercury is supplied from a heated elemental Hg reservoir. Figure 4 shows a schematic of the two-zone reactor with the heated Hg and growth zones. It also shows how the DMCd is introduced separately from the dopants and downstream of the Hg zone to prevent detrimental pre-reactions.

Alloy composition and uniformity control is achieved by means of the interdiffused multilayer process (IMP).[2] This technique separates the growth of the CdTe and the HgTe binaries into separate cycles such that each can be deposited under more ideal growth conditions. These can then be grown as alternating thin layers which interdiffuse rapidly to form a uniform alloy due to the high interdiffusion coefficients of the binary compounds. The relative ratio of binary layer thickness directly controls the composition (and hence the band gap) of the CMT layers, following:

$$\text{Cadmium alloy fraction, } x = t_{CdTe} / (t_{CdTe} + t_{HgTe}).$$

The IMP technique enables the easy production of heterostructures because only changes in the relative binary growth periods were required in order to control the composition within a structure, rather than having to change the growth conditions.

MOVPE growth is performed onto either the Cd(Zn)Te family or GaAs or GaAs:Si substrates. The former offer a potentially lattice-matched growth substrate for minimising interfacial misfit dislocations. However, nonuniformities arising from the high segregation coefficient of Zn in CdZnTe means that in practice it is very difficult to grow significant areas which are truly lattice matched. The high costs and poorer crystalline quality of the II/VI family of substrates have stimulated research into growth on alternative substrates such as GaAs or GaAs:Si, which are available in larger sizes, such as a 3" diameter. The GaAs:Si substrate route offers the added advantage of preventing thermal expansion mismatch when cooling large hybridised arrays, thereby eliminating the need for substrate removal of the array component in the finished hybrid, provided the design of the detector dewar appropriately addresses the thermal expansion coefficients of the array substrate components.

MOVPE growth is generally performed onto substrates which are misoriented from the (100) direction by between 2–8° to minimise the density of pyramidal hillock growth

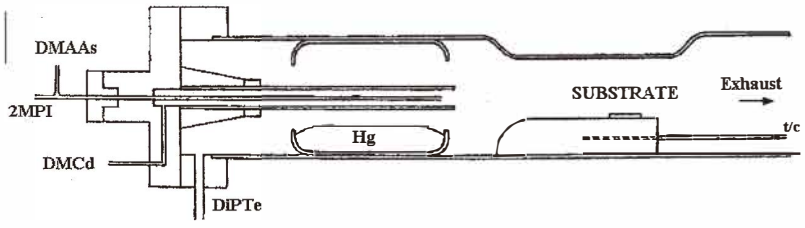

Fig. 4. Schematic showing the MOVPE reactor design.

defects. On II/VI substrates, the 20–100 defects cm^{-2} are thought to be linked to Te inclusions and imperfections at the growth interface. On GaAs, substrate preparation and CdTe buffer growth conditions exert a strong influence on the suppression of hillocks. We have found that by growing the CdTe buffer layers at lower temperatures (≈300°C) using methylallyl tellurium (MATe), hillock densities can be suppressed to 0–5 cm^{-2} on GaAs.[3]

The 77 K electrical properties of undoped layers, grown at ~350°C with a Hg overpressure of ≈0.02 atm, are dominated by ≈5×10^{16} cm^{-3} metal site vacancies. These defects can be removed by isothermal annealing at ≈200–250°C which converts the layer properties to n-type due to a low residual donor concentration of ≈$2–4\times10^{14}$ cm^{-3}.

The incorporation of extrinsic dopants into the CMT lattice enables the production of heterojunction devices which do not depend on metal vacancy control.

Arsenic doping is achieved using either *tris*-dimethyl amino arsine (DMAAs) or phenyl arsine which can produce a range of doping concentrations from as low as 10^{15} cm^{-3} to ≈5×10^{17} cm^{-3}. The key to achieving dopant activity of the potentially amphoteric Group V elements is the use of Cd-rich conditions during the CdTe IMP cycles. By ensuring that the DMCd: DiPTe ratio is greater than ~1.2, good activation efficiencies (~100%) are obtained (see Fig. 5), implying the correct location of As atoms onto Te lattice sites.[4] Layers (x~0.3) doped using DMAAs have demonstrated radiatively limited lifetimes at 77 K and are found to be consistent with very low Shockley-Read trap densities (~5×10^{10} cm^{-3}).[5]

Donor doping is achieved using either 2-methyl propyl iodide (2MPI) or ethyl iodide (EtI) which allows control of the donor concentration in the range from mid-10^{14} cm^{-3} to mid-10^{17} cm^{-3} with a high activation efficiency (see Fig. 6).[6] The electrical characteris-

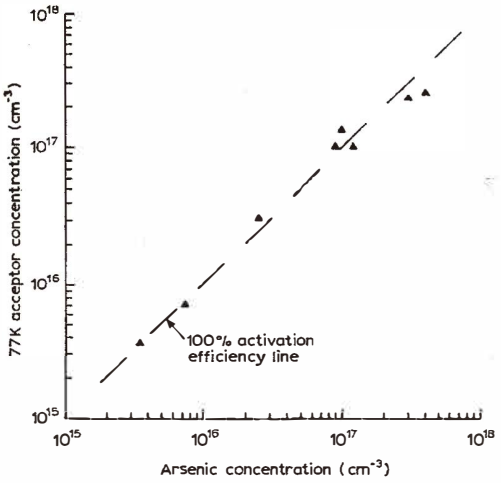

Fig. 5. 77 K Hall acceptor concentration, after Hg anneal, as a function of the arsenic concentration in CMT layers doped using phenyl arsine.

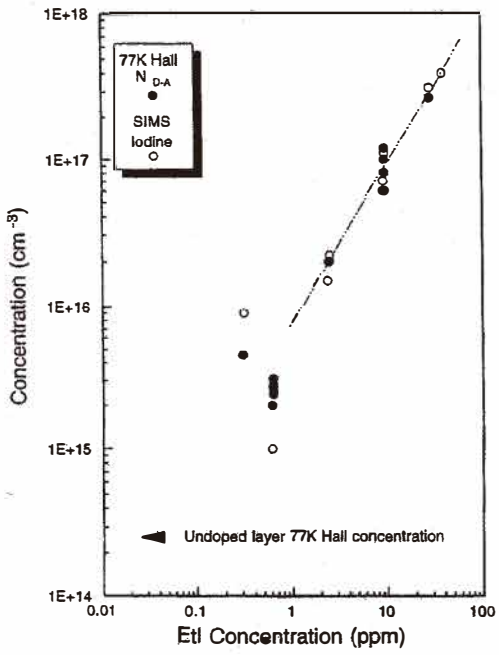

Fig. 6. Calibration curve obtained with EtI.

tics of I-doped layers exhibit 77 K electron mobilities close to In-doped LPE (see Fig. 7). I-doped layers ($\approx$2–3$\times10^{15}$ cm^{-3}) demonstrate minority carrier lifetimes of 250 ns, which are consistent with band-to-band recombination processes.

The growth of fully doped heterostructures involving changes in composition and doping can be performed once both acceptor and donor doping capabilities have been demonstrated. Research has concentrated on producing Auger-suppressed, nonequilibrium devices and multilayer equilibrium MW devices. A SIMS profile of the latter, Fig. 8, reveals the alloy fraction, x and the dopant impurity concentrations throughout the depth of the epitaxially grown MW device structures. Interdiffusion at the growth temperature leads to heterointerfaces with a width of 0.8 μm.

The multilayer device structures lend themselves to a simple process route for flip-chip-bonded, mesa-etched diode arrays which can be manufactured on a wafer scale. Although much of the development work to date has been performed on 1" substrates, the MOVPE growth is being scaled up to 3" or 4" substrates for larger scale manufacturing programmes.

4. Indium Antimonide

Interest in indium antimonide (InSb) for large area focal plane arrays has been generated by the availability of high-quality 3" substrate materials. Compared with the

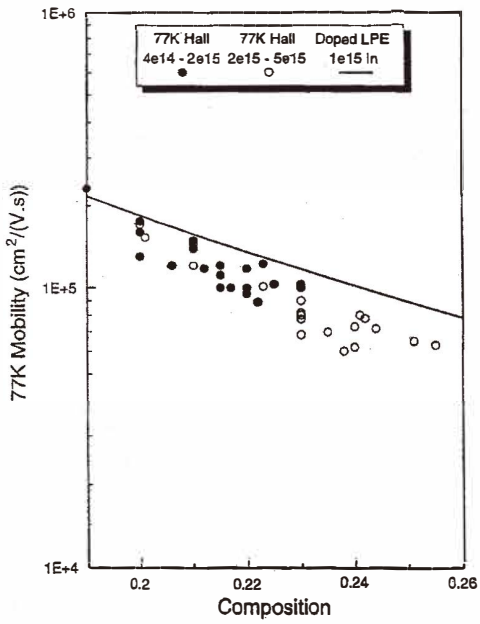

Fig. 7. Variation of 77 K mobility as a function of composition for two ranges of excess donor concentration.

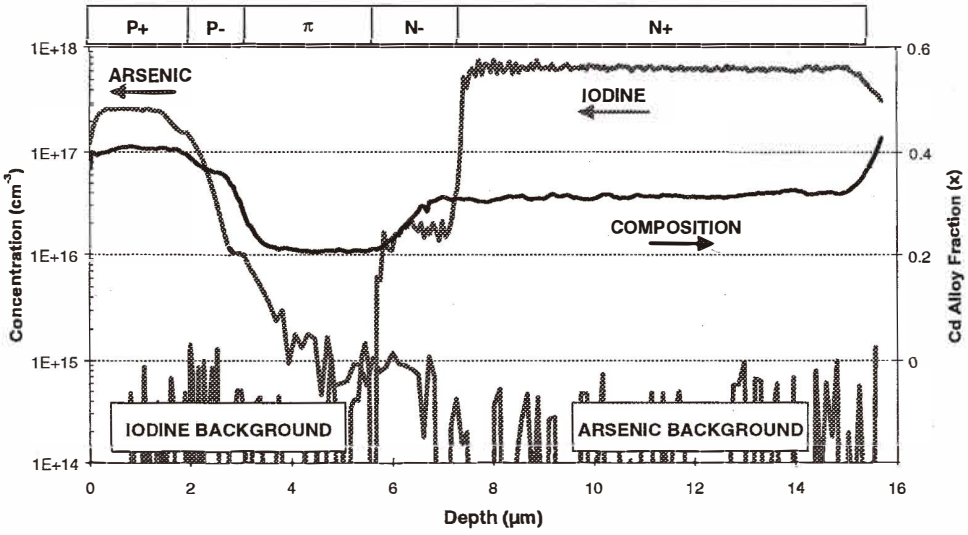

Fig. 8. SIMS As, I and composition profiles of a $\underline{p}^+\underline{p}^-\pi\underline{n}^-\underline{n}^+$ structure designed for MW detection operating at 240 K.

CMT LPE technology, it offers potential advantages in terms of manufacturing costs and uniformity, and compared with the CMT MOVPE technology, it offers superior uniformity albeit at a fixed wavelength. Further economies are achieved over LPE by wafer scale processing up to hybridisation, when the wafers are sawn into individual arrays before bump bonding to a silicon read-out circuit.

320×256 pixel arrays at 30 μm pitch and full TV 640×512 pixels at 24 μm pitch are under development, with the individual diodes (pixels) defined by mesa etching, using a process very similar to that for MOVPE multilayers. Indium bumps are applied for hybridisation by bump bonding. Figure 9 shows an example of an InSb array.

Unlike CMT, InSb is of fixed composition and hence provides a uniform cut-off wavelength of 5.5 μm at 80 K (CMT requires a cold filter to define a uniform cut-off over large areas). Detectors fabricated from this material, in the main, are formed by ion implantation or diffusion and require thinning to within a diffusion length of the junction (less than about 20 μm). Passivation of this back surface is critical in order to reduce surface recombination of the photogenerated carriers.

In collaboration with DERA Malvern, we have developed a novel approach in order to overcome the severity of the thinning requirement. Use is made of a degenerately doped substrate for the growth of a p-i-n diode structure by molecular beam epitaxy (MBE). The degeneracy (Moss-Burstein shift) shifts the cut-off wavelength of the substrate down to around 3 μm, which presents a window covering the 3–5 μm band. Photons in this band pass through to the active i-region before being absorbed. This is illustrated in Fig. 10 where a substrate doping of 6×10^{17} cm^{-3} is used.

Substrate thinning is only required in order to reduce absorption by the free electrons in the conduction band, and a final thickness of up to 100 μm is adequate. Unlike conventional InSb detectors, the thickness uniformity of the final substrate thickness does not significantly affect array uniformity. A substrate doping level of 2×10^{18} cm^{-3} has a cut-on wavelength close to 3 μm, allowing absorption at the junction in the 3–5.5 μm

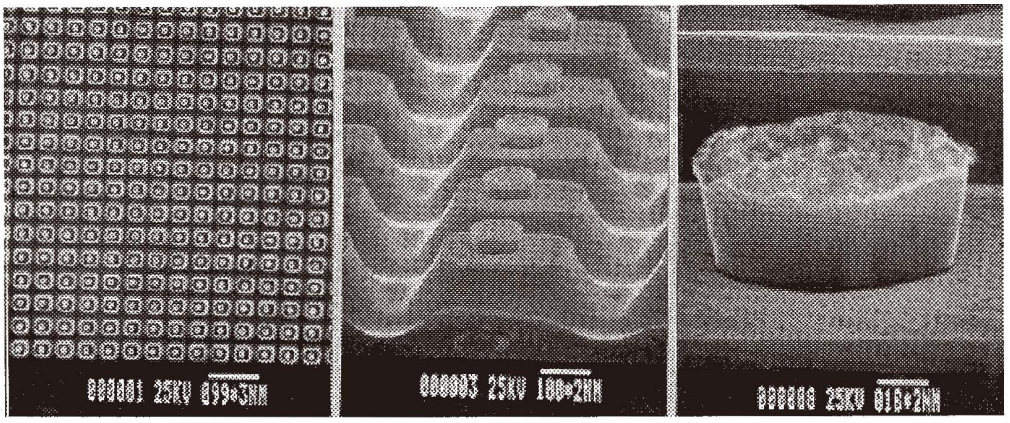

Fig. 9. InSb array process.

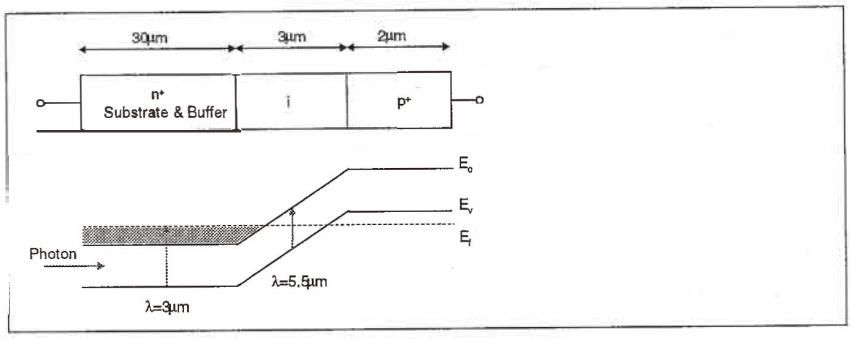

Fig. 10. InSb detector structure.

window. A variation in substrate thickness of several tens of microns has a minimal effect on this free carrier absorption (*e.g.*, a change in thickness from 60 μm to 120 μm increases absorption by only 3%).

Similarly, the surface is remote from the active junction such that electrical passivation of this surface is not necessary. The active region is automatically passivated at the growth interface to the highly doped buffer layer on the growth substrate. With this epitaxial interface, the use of an insulator on the semiconductor surface is unnecessary, as in a conventional InSb diode structure, and consequently the possibility of electronic traps is avoided in the region of the semiconductor-insulator interface; these can be associated with memory effects in the surface recombination rates leading to the possibility of long-term artefacts which can be 'burned-in' to the infrared image, for example by exposure of the array to an image hot-spot. The new MBE InSb arrays are free of such artefacts.

An additional advantage of the MBE devices is the designed, small thickness of the absorber layer in comparison with the thickness of conventional devices, which reduces the volume available for the thermal generation of dark current. The quality of infrared imagery produced remains fairly constant for operating temperatures up to 100 K, in contrast to conventional devices in which performance degrades more rapidly with increasing operating temperature.

Detectors with less than 0.3% defective pixels have been produced and a typical image is shown in Fig. 11.

5. Uncooled Thermal Detector Arrays

Our uncooled thermal detector arrays all utilize the pyroelectric effect (the temperature-dependent polarisation of a dielectric material) to generate an electrical signal from the incoming infrared image. Much attention has been paid to the selection and development of high-performance pyroelectric materials (high pyroelectric response, low dielectric loss) in the physical forms required for imaging arrays.[7,8]

Fig. 11. Typical image from InSb array.

Two forms of the materials have been used. These are hot-pressed bulk ceramic and sol-gel or sputtered thin films. For each material, technologies have been developed to fabricate arrays of elements on a pitch of 100 μm or less. These elements are designed for maximum performance by matching the thermal time constant of the pixel to the operating frequency of the array, typically 100 Hz.[9,10] This requires a micromachined element construction, intimately connected to a buffer amplifier contained in each pixel of a custom read-out circuit.

The array is operated in a camera incorporating a chopper, which scans over the array in synchronisation with the raster readout of the array. The data from the resulting 'open' and 'closed' fields are stored and processed in real time to generate the image displayed in standard TV format.[11] Performance enhancement measures such as microscan may be included in the camera.

Our simplest array is a 100×100 pixel array, fabricated from a monolithic piece of modified PZT (lead zirconate titanate) ceramic of 40 μm thickness, without reticulation, which is flip-chip bonded to its readout circuit on a pitch of 100 μm. The principal application for this array has been in a helmet-mounted camera for firefighters. This was the first commercial solid-state pyroelectric camera, and benefits in this application from very good performance stability across a wide temperature range. The sensitivity achieved is 200 mK NETD in f/1 at a 50 Hz field rate, although the MTF, as is characteristic of an unreticulated array, is relatively poor.

The most advanced array in production (Fig. 12) has 256×128 elements, fabricated from PST (lead scandium tantalate) ceramic only 16 μm thick. Laser micromachining is used to reticulate the PST array for improved thermal isolation between the elements, which leads to improved spatial resolution in the thermal image. This array is used in sights such as the LION handheld imager (Fig. 13), and a typical image is shown in Fig. 14. The use of the more advanced PST material, which is an induced pyroelectric optimised for near-room-temperature operation, combined with reduced ceramic thickness, vacuum packaging, and laser reticulation, enables this detector to outperform the earlier 100×100 array even with its reduced pitch of 56 μm. Typical NETD is 100 mK with an MTF of 40% at the Nyquist frequency.

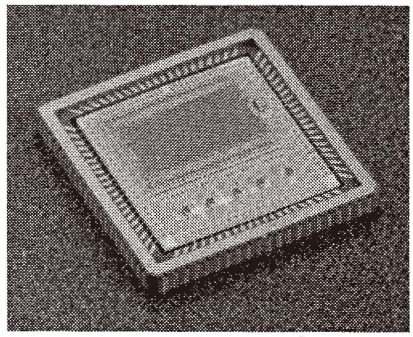

Fig. 12. 256×128 pyroelectric array.

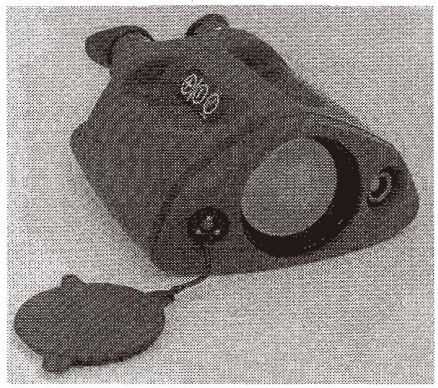

Fig. 13. LION hand held imager.

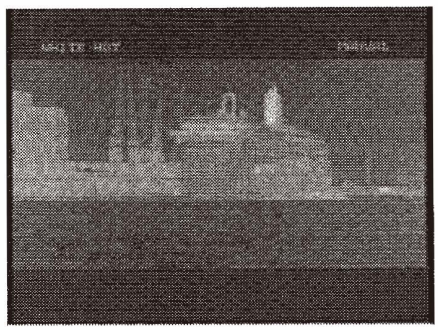

Fig. 14. Typical pyroelectric 256×128 image.

The same technology has been used to demonstrate 384×288 element arrays, but a more advanced approach will be implemented to enable this size of array to achieve higher sensitivity than its predecessors, at reduced pitch (40 μm).

In uncooled pyroelectric arrays, the key to improving performance further is to reduce the thermal mass of the detecting element, thus increasing the temperature change induced by a given incident infrared flux. This is achieved by the use of thin film materials in microbridge structures, which also achieve MTF at the theoretical limit when packaged in vacuum. Submicron-thickness pyroelectric films of both PST and PZT have been employed in microbridge arrays which are currently under development, though the next planned product development is a PST array. The predicted NETD of this array is 30 mK in f/1 at 50 Hz.

6. Summary

Whereas LPE-grown CMT on CdZnTe substrates continues to supply state-of-the-art arrays for second-generation thermal imagers, the trend towards large-format 2D arrays for high-performance imaging has stimulated the development of semiconductor materials and device structures which offer affordability and low defect density with at least 3" diameter wafer sizes. The scope of detector development includes the MBE growth of InSb to provide dedicated 3–5 μm arrays. In parallel, the MOVPE technique provides a flexible tool for the manufacturing of CMT detectors over an extended wavelength range, including short-wave applications below 2 μm. A multilayer capability has been demonstrated using MOVPE, extending at least to five-layer structures, and this has laid a foundation for multiband array structures.

Pyroelectric materials present many difficulties for the engineering of thin-film microbridges on Si read-out circuits, but nevertheless offer the highest theoretical sensitivity among the known bolometer materials, and the potential to approach the current performance of cooled arrays within one or two years.

Acknowledgements

The LION hand held imager illustrated in Fig. 13 is shown by kind permission of its manufacturers, Delft Signaal Optronics. The authors wish to thank our collaborators in the UK Defence Evaluation and Research Agency for their valuable contributions to the work described, and to acknowledge the financial support of the UK Ministry of Defence in many areas.

References

1 P. Capper: Narrow-Gap II-VI Compounds for Optoelectronic and Electromagnetic Applications (Chapman & Hall, London, 1997).
2 J. Tunnicliffe, S. J. C. Irvine, O. D. Dosser and J. B. Mullin: J. Cryst. Growth **68** (1984) 245.
3 A. Wasenczuk, A. F. W. Willoughby, P. Mackett, E. O'Keefe, P. Capper and C. D. Maxey: J. Cryst. Growth **159** (1996) 1090.
4 P. Capper, P. A. C. Whiffin, B. C. Easton, C. D. Maxey and I. Kenworthy: Mater. Lett. **6** (1988) 365.
5 C. D. Maxey, C. L. Jones, N. E. Metcalfe, R. A. Catchpole, N. T. Gordon, A. M. White and C. T. Elliott: Proc. SPIE **3122** (1997) 453.

6 C. D. Maxey, C. L. Jones, N. E. Metcalfe, R. Catchpole, M. R. Houlton, A. M. White, N. T. Gordon and C. T. Elliott: J. Electron. Mater. **25** (1996) 1276.
7 R. W. Whatmore: Rep. Prog. Phys **49** (1986) 1335–1386.
8 A. Patel and J. Obhi: GEC J. Res. **12** (1995) 141–152.
9 N. M. Shorrocks, A. Patel, M. J. Walker and A. D. Parsons: Microelectron. Eng. **29** (1995) 59–66.
10 S. G. Porter: Ferroelectrics **33** (1981) 193–206.
11 R. K. McEwen and P. A. Manning: Proc. SPIE **3698** (1999) 322–337.